

## Electronic Supplementary Information

### Impact of tensile and compressive forces on hydrolysis of cellulose and chitin

Hirokazu Kobayashi<sup>\*1</sup>, Yusuke Suzuki<sup>1,2</sup>, Takuya Sagawa<sup>1,3</sup>, Kyoichi Kuroki<sup>1,2</sup>, Jun-ya Hasegawa<sup>1</sup>, Atsushi Fukuoka<sup>\*1</sup>

<sup>1</sup>*Institute for Catalysis, Hokkaido University, Kita 21 Nishi 10, Kita-ku, Sapporo, Hokkaido 001-0021, Japan.*

<sup>2</sup>*Graduate School of Chemical Sciences and Engineering, Hokkaido University, Kita 13 Nishi 8, Kita-ku, Sapporo, Hokkaido 060-8628, Japan.*

<sup>3</sup>*Department of Industrial Chemistry, Faculty of Science, Tokyo University of Science, 12-1 Ichigaya-funagawara-machi, Shinjuku-ku, Tokyo, 162-0826, Japan.*

E-mail: kobayashi.hi@cat.hokudai.ac.jp (H.K.); fukuoka@cat.hokudai.ac.jp (A.F.)

**Total –17 pages, 13 figures, 8 tables–**

Analysis of products .....	S2
Fig. S1 .....	S2
Fig. S2 .....	S2
Fig. S3 .....	S3
Fig. S4 .....	S3
Table S1 .....	S4
Table S2 .....	S5
Determination of collision velocity of ball in planetary milling .....	S6
Fig. S5 .....	S6
Collision of a ball to a biomass sample .....	S8
Fig. S6 .....	S8
Fig. S7 .....	S8
Table S3 .....	S9
Validation and benchmark of DFT calculations .....	S10
Fig. S8 .....	S10
Fig. S9 .....	S10
Table S4 .....	S11
Additional information for DFT calculations .....	S12
Fig. S10 .....	S12
Fig. S11 .....	S12
Fig. S12 .....	S13
Fig. S13 .....	S13
Table S5 .....	S14
Table S6 .....	S15
Table S6 .....	S16
Table S8 .....	S17

## Analysis of products

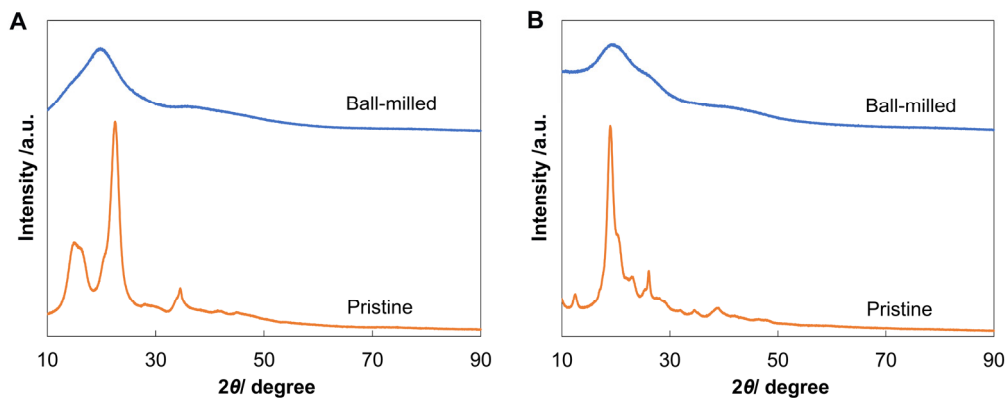


**Fig. S1.** XRD patterns of (A) cellulose and (B) chitin.

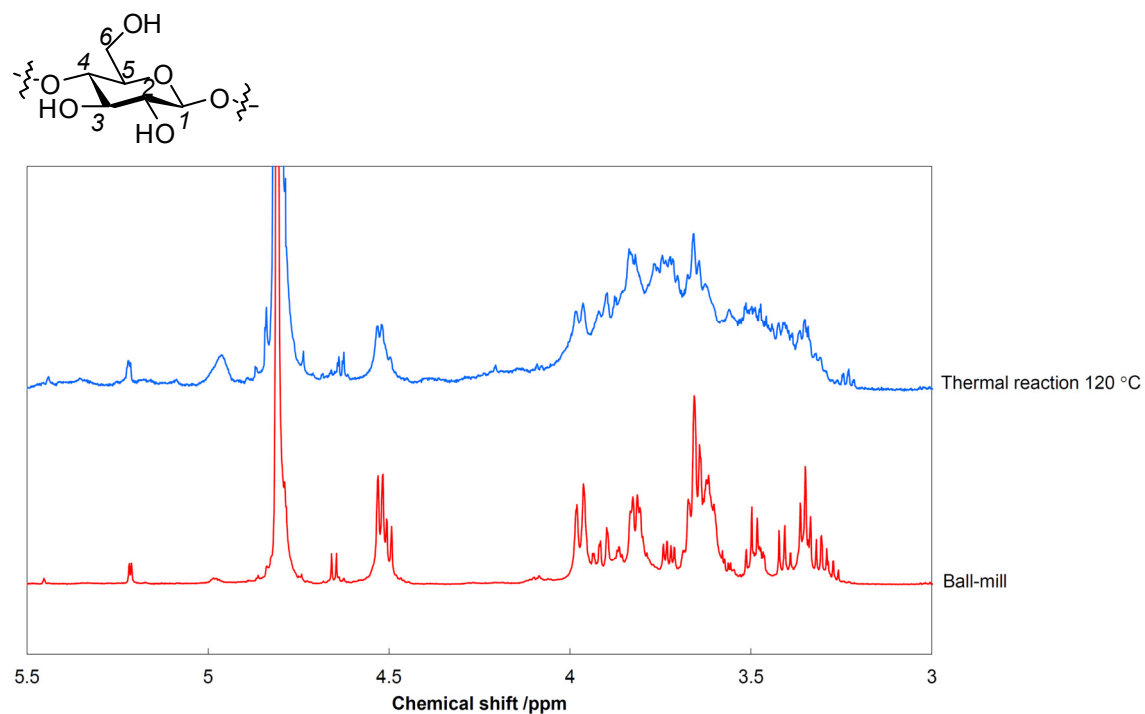


**Fig. S2.** <sup>1</sup>H NMR spectra for the cellulose hydrolysates and standard cello-oligosaccharides.

Reaction time 12 h.

$\delta$  (ppm) = 5.4 (H1 of 1,6-anhydro- $\beta$ -glucose unit); 5.2 ( $\alpha$ -reducing end H1); 4.95 ( $\alpha$ -1,6-H1); 4.65 ( $\beta$ -reducing end H1); 4.5–4.6 (inner  $\beta$ -1,4-H1); 4.1 (possibly H6 of 1,6-anhydro- $\beta$ -glucose unit). Assignments: J. Beltramini *et al.*, *Green Chem.* **15**, 2761–2768 (2013); S. Shoda *et al.*, *Tetrahedron Lett.* **50**, 2154–2157 (2009).

The very complicated peaks at 3.2–4.1 ppm for the thermal-reaction sample is due to the presence of various kinds of glycosidic bonds. A broad peak at 5.3 ppm is derived from H1 of  $\alpha$ -1,3- and  $\alpha$ -1,2-bonds. We have previously analysed dimer products, and found any glycosidic bonds from  $\alpha$ -1,1 to  $\beta$ -1,6 (A. Fukuoka *et al.*, *Bull. Chem. Soc. Jpn.* **93**, 273–278 (2020)).

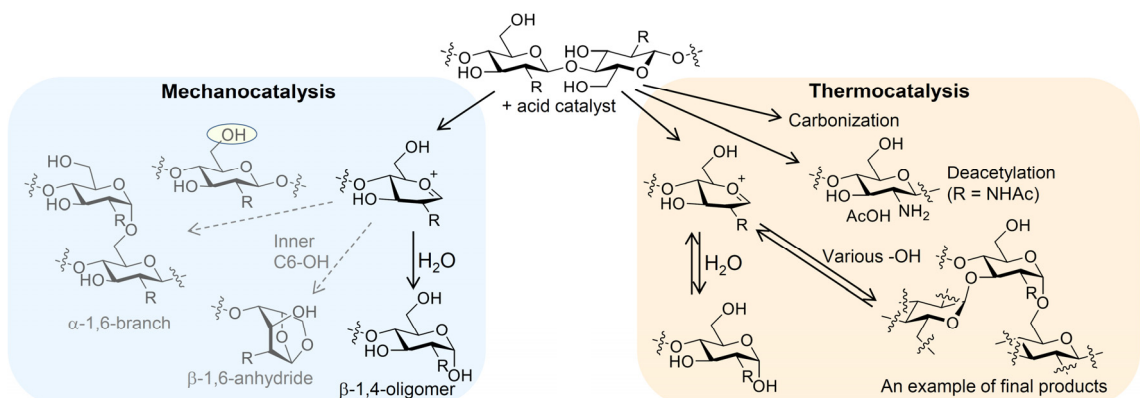


**Fig. S3** Hydrolysis of cellulose and chitin with physisorbed water in the absence of solvent.

In the thermal reactions, the reaction with little water, namely the same as ball-milling conditions, eventually gives randomly connected glucose oligomers and also facilitates the formation of carbonaceous materials.

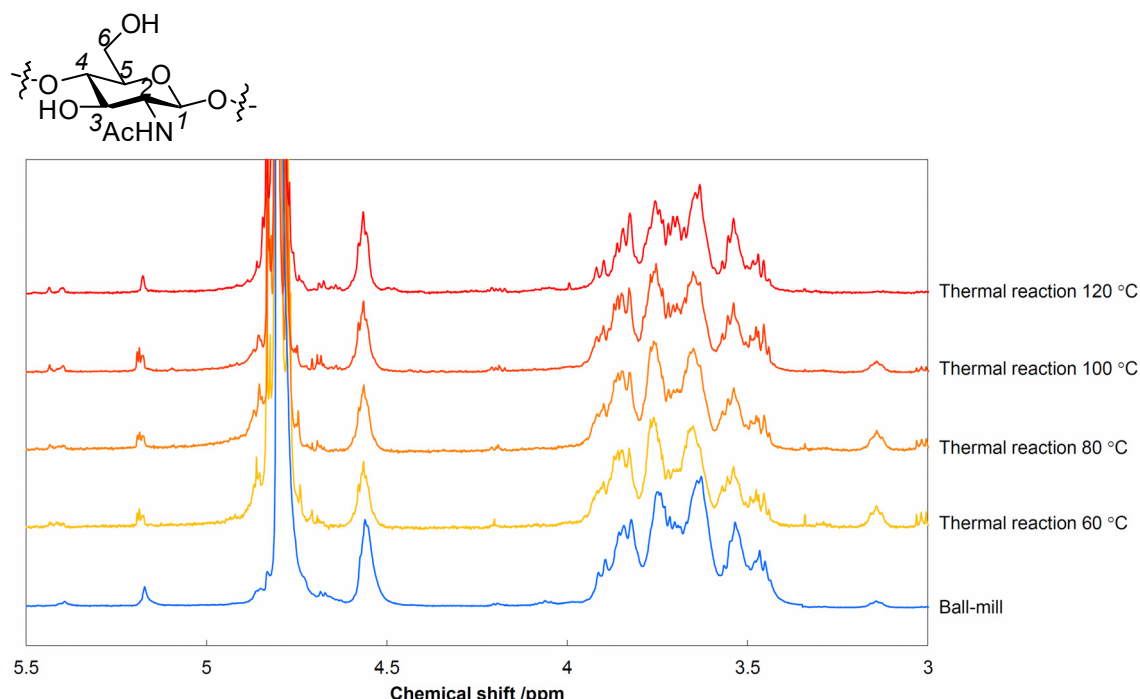


**Fig. S4.** <sup>1</sup>H NMR spectra for the chitin hydrolysates and standard chitin-oligosaccharides. Reaction time 12 h.

$\delta$  (ppm) = 5.4 ( $\alpha$ -1,6-H1 or H1 of 1,6-anhydro- $\beta$ -NAG unit); 5.2 ( $\alpha$ -reducing end H1); 4.8 (HDO); 4.7 ( $\beta$ -reducing end H1); 4.6 (H3 of 1,6-anhydro- $\beta$ -NAG unit); 4.55 (inner  $\beta$ -1,4-H1); 4.2 (H6 of 1,6-anhydro- $\beta$ -NAG unit); 3.4–3.9 (H2–H6). Assignments: M. Yabushita *et al.*, *ChemSusChem* **8**, 3760–3763 (2015).

NMR spectra of chitin-derived oligomers are more complicated than that derived from cellulose, because chitin originally contains two types of monomer units, NAG and glucosamine.

**Table S1.** Thermal hydrolysis of H<sub>3</sub>PO<sub>4</sub>-impregnated cellulose.<sup>a</sup>

Time	Photo of the product	Product yield	
		Glucose /C%	Oligomers /C%
1		2.7	17
3		3.2	19
6		3.9	22
12		2.8	18

<sup>a</sup>Cellulose was milled by planetary milling, followed by the impregnation of H<sub>3</sub>PO<sub>4</sub> (S/C =5, mol/mol). The sample was treated in a high-pressure glass flask at 120 °C for a designated time.

**Table S2.** Thermal hydrolysis of H<sub>3</sub>PO<sub>4</sub>-impregnated chitin.<sup>a</sup>

Temp.	Time	Photo of the product	Product yield		
			NAG /C%	Oligomers /C%	AcOH /mol%
120	0.5		2.3	15	2.4
120	1		2.6	17	2.9
120	3		3.7	29	24
120	6		1.3	28	18
120	12		0.4	19	39
60	12		1.1	6.9	<1
80	12		1.3	7.7	1.4
100	12		2.9	17	3.4

<sup>a</sup>Chitin was milled by planetary milling, followed by the impregnation of H<sub>3</sub>PO<sub>4</sub> (S/C =5, mol/mol). The sample was treated in a high-pressure glass flask at the designated temperature for a certain time.

## Determination of collision velocity of ball in planetary milling

The ball was regarded as a mass point for convenience, as the size (5 mm) was much smaller than the pot diameter (74.8 mm). Fig. S5A depicts the moment when the ball just departing from the pot wall during milling, which is denoted detachment. The pot (radius  $r$ ) is rotating at an angular velocity of  $\omega$ , and it has a revolution orbit with a radius of  $R$  and an angular velocity of  $\Omega$ . To describe this system, a Cartesian coordinate was designed to be an inertial frame of reference. This can avoid the appearance of a fictitious force, Coriolis force. The original point  $O$  was located at the centre of the revolution orbit, and the  $x$ -axis passed through the centre of the pot at the time of the detachment.

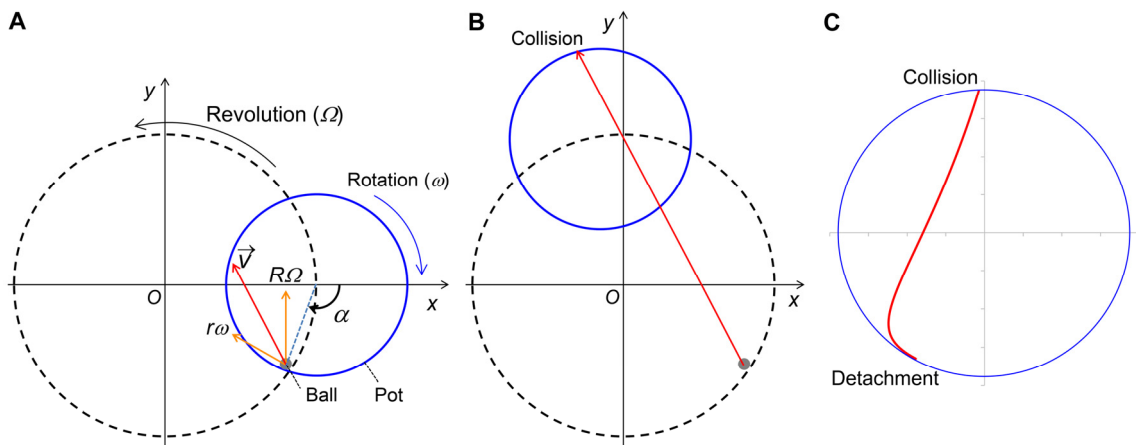


**Fig. S5.** Model for calculating ball motion in a planetary mill. (A) Motion vectors of the ball at the detachment, (B) collision of the ball to the pot wall, (C) resulting trajectory of the flying ball shown in an internal coordinate of the pot for our case. The blue circles indicate the inner wall of the pot, and the dashed lines show the revolution orbits of the pot.

At the detachment event (Fig. S5A),  $\alpha$  is defined as an angle between the  $x$ -axis and the vector from the centre of the pot to the ball. Then, the coordinate of the ball is described as  $(R + r \cos \alpha, -r \sin \alpha)$ , and  $x$  and  $y$  components of the velocity,  $v_x$  and  $v_y$ , are  $-r\omega \sin \alpha$  and  $R\Omega - r\omega \cos \alpha$ , respectively. The angle  $\alpha$  is such that the ball has no vector component of acceleration toward the pot wall, thus giving eq. S1. In our case,  $\alpha$  is  $118^\circ$  ( $2.07$  rad) at  $r = 3.74 \times 10^{-2}$  m,  $R = 5.25 \times 10^{-2}$  m,  $\omega = 42.8$  rad s $^{-1}$ , and  $\Omega = 52.4$  rad s $^{-1}$ .

$$-R\Omega^2 \cos \alpha = r\omega^2 \quad (\text{S1})$$

After the detachment, the ball flies in a uniform linear motion at the velocity described above.

This motion provides a coordinate of the ball ( $R + r \cos \alpha - r\omega t \sin \alpha, -r \sin \alpha + (R\Omega - r\omega \cos \alpha)t$ ), where  $t$  indicates the elapsed time from the detachment. Meanwhile, the pot revolves around  $O$ , giving a coordinate of the pot centre ( $R \cos \Omega t, R \sin \Omega t$ ).

The ball eventually hits the wall of the pot at some point, which is named collision (Fig. S5B). At the collision, the distance between the centre of the pot and the ball is the same as the radius of the pot ( $r$ ), holding eq. S2 true. This equation might not be analytically soluble, and therefore we numerically calculated coordinates of the ball and the pot centre and their distance at every 10  $\mu$ s using the parameters for our case. The trajectory of the ball in the pot (Fig. S5C) indicates that the ball hits the wall in a nearly vertical direction after the pot rotating 104° (1.81 rad). The relative velocity of the ball to the pot wall at the collision point is 4.08 m s<sup>-1</sup>. This value was used as a model collision speed in our planetary milling for further study.

$$[R + r \cos \alpha - r\omega t \sin \alpha - R \cos \Omega t]^2 + [-r \sin \alpha + (R\Omega - r\omega \cos \alpha)t - R \sin \Omega t]^2 = r^2 \quad (\text{S2})$$

### Collision of a ball to a biomass sample



**Fig. S6.** Photograph for an alumina ball with cellulose powder after milling. Scale bar 1 mm.

The thickness of cellulose on the ball was roughly 0.05–0.15 mm. The pot wall had a similar thickness of cellulose. Therefore, a collision of a ball sandwiches roughly 0.1–0.3 mm thickness of cellulose. Taking into account further margin, it would be 0.08–0.4 mm. Note that we used only 5 g of cellulose in a pot (250 mL) to avoid absorbing the collision shock by excess cellulose.

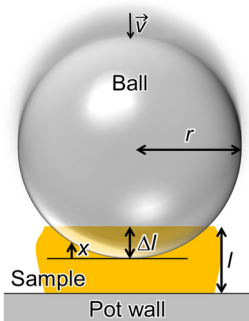


**Fig. S7.** Schematic for collision of the ball to a cellulose/chitin particle on the pot wall. The transparent orange rectangle indicates sample.

For the analytical force calculations (Fig. S7), using  $x$  as the height from the bottom of the ball, eq. S3 shows the differentiation of contact cross-sectional area between the ball and the sample at  $x$ . Thus, the force applied to the ball can be approximated by eq. S4 using eq. S3, Young's modulus ( $Y$ ), and the thickness of the sample ( $l$ ), where  $\Delta l$  describes the deformation length of the sample at the centre at a certain moment. Integral of eq. S4 from  $\Delta l = 0$  to some  $\Delta l$  gives energy consumption ( $\Delta E$ ) of the ball used for deformation of the sample (eq. S5). The energy usage becomes equal to the original kinetic energy of the ball at a particular  $\Delta l$ , which is the point for the maximum deformation of the sample.

$$\frac{dS}{dx} = 2\pi(r - x) \quad (S3)$$

$$F = \int_0^{\Delta l} 2\pi(r - x) \cdot Y \frac{\Delta l - x}{l} dx = \frac{\pi Y}{l} (r\Delta l^2 - \frac{1}{3}\Delta l^3) \quad (S4)$$

$$\Delta E = \int_0^{\Delta l} F dx = \frac{\pi Y}{l} (\frac{r}{3}\Delta l^3 - \frac{1}{12}\Delta l^4) \quad (S5)$$

**Table S3.** Simulation of ball collision to cellulose particle by a finite element method.<sup>a</sup>

Collision angle <sup>b</sup>	Friction coefficient	Maximum stress /GPa	
		Compression	Tension
90°	0	4.9	0.66
45°	0	3.1	0.63
45°	0.4	3.3	0.96
45°	0.6	3.7	1.3
30°	0	2.3	0.48
30°	0.2	2.3	0.62
30°	0.4	2.5	0.91
30°	0.6	2.5	1.5
15°	0.6	1.3	0.56

<sup>a</sup>Young's modulus: isotropically 137 GPa for cellulose; cellulose thickness 0.4 mm. <sup>b</sup>Angle between ball velocity and collision surface of cellulose.

## Validation and benchmark of DFT calculations

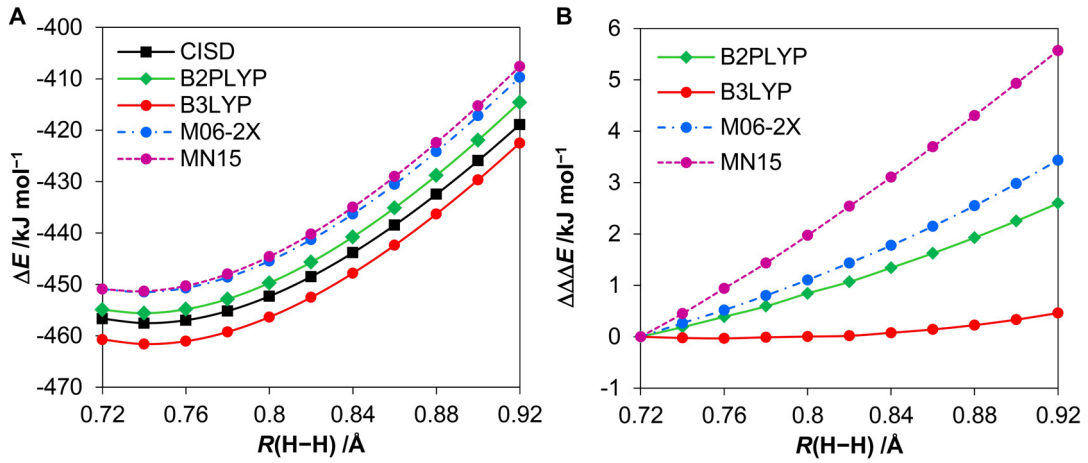


**Fig. S8.** (A) Potential energy of H<sub>2</sub> at each distance and (B) derivative of difference from CISD values. Basis set: aug-cc-pV5Z. CISD works as the full configuration interaction (full-CI) in the two-electron system.

B3LYP gives  $\Delta\Delta\Delta E$  values of almost zero in the full range in (B), which means that shape of the potential curve is very similar to that of CISD.

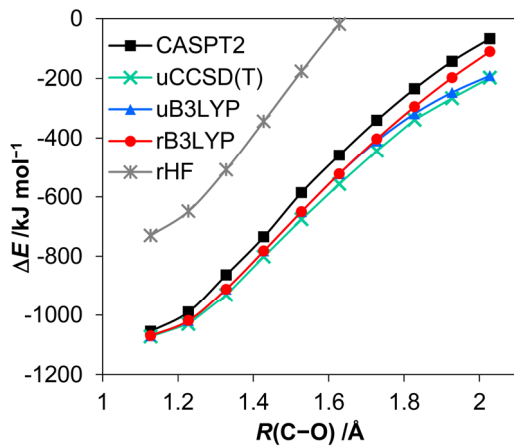


**Fig. S9.** Potential energy of CO at each distance. Basis set: aug-cc-pVQZ. For CASPT2, ten electrons with eight orbitals (2s $\sigma$ , 2p $\sigma$ , 2×2p $\pi$ , and their anti-bonding orbitals) were included in the active space. Perturbation was considered for the configurations with CI coefficients larger than 0.01.

**Table S4.** Benchmark test of DFT functionals and basis sets in the bond elongation and protonation of dimethyl ether.

Functional	Basis set	Electronic energy ( $\Delta$ from the CCSD(T) data) /kJ mol <sup>-1</sup>					
		Elongation <sup>a</sup>		Protonation <sup>b</sup>		Elongation of protonated form <sup>ab</sup>	
CCSD(T)	aug-cc-pVTZ	+15.2		-823.3		+9.9	
B3LYP	6-31+G(d,p)	+15.2 (0.0)		-821.5 (+1.8)		+9.3 (-0.6)	
B3LYP	aug-PC-1	+15.5 (+0.3)		-811.2 (+12.1)		+9.4 (-0.5)	
CAM-B3LYP	aug-PC-1	+16.1 (+0.9)		-806.0 (+17.3)		+10.0 (+0.1)	
M06-2X	aug-PC-1	+16.4 (+1.2)		-809.6 (+13.7)		+10.3 (+0.4)	
MN15	6-31+G(d,p)	+15.4 (+0.2)		-820.7 (+2.6)		+9.6 (-0.3)	
MN15	aug-PC-1	+15.5 (+0.3)		-810.8 (+12.5)		+9.6 (-0.3)	
$\omega$ B97XD	aug-PC-1	+16.6 (+1.4)		-819.2 (+4.1)		+10.3 (+0.4)	

<sup>a</sup>Distance between the two C atoms in a dimethyl ether molecule were increased by 0.2 Å from the equilibrium positions determined by respective methods. <sup>b</sup>The O atom was protonated.

## Additional information for DFT calculations



**Fig. S10.** Syn- and anti-periplanar conformations for the cleavage of glycosidic bonds.

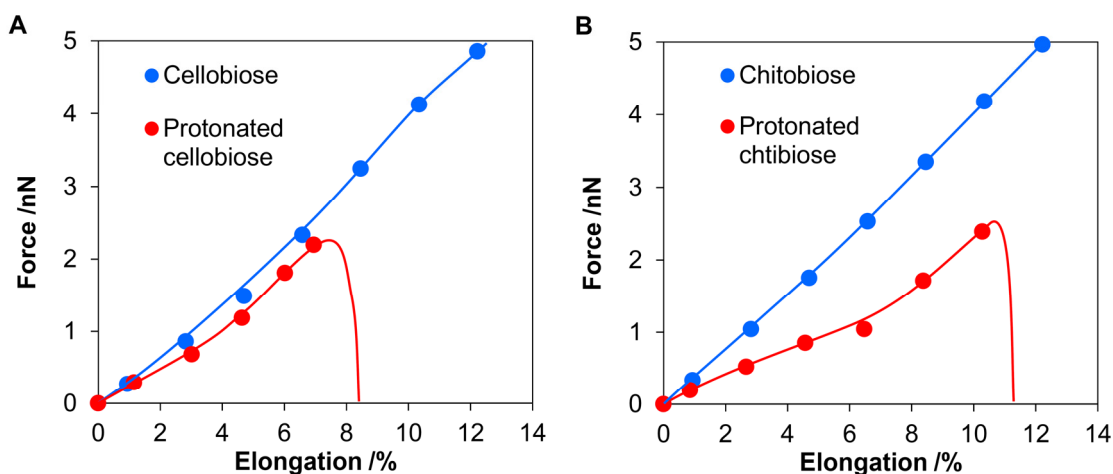


**Fig. S11.** Forces required for the stretch of (A) cellobiose and (B) *N,N'*-diacetylchitobiose. Blue: pristine molecules; red: protonated ones.

Cellobiose and *N,N'*-diacetylchitobiose molecules protonated at the glycosidic bonds needed smaller forces for the stretching. Pulling the molecules with more than 2 nN of forces cleaved their glycosidic bonds. In the case of cellobiose, this reaction unexpectedly produced a glucose molecule and a protonated condensed ring product (Fig. S12). We have not observed related products in real experiments. Theoretical formation of the strange product was not due to lack of long-range correction of B3LYP, because  $\omega$ B97XD also gave the same products. Instead, the major cause would be the use of a free proton that activates glycosidic bond too strongly and lack of thermal effect dissociating glycosidic bonds before the force directly breaks the bond. We have found that protonated cellobiose with no tensile forces changes the conformation from armchair to  $E_3$  with 7.4 kJ mol<sup>-1</sup> of activation energy (TS 52i cm<sup>-1</sup>). The product spontaneously cleaved its glycosidic bond to produce an oxocarbenium ion. Therefore, the direct mechanical dissociation is unlikely very important.

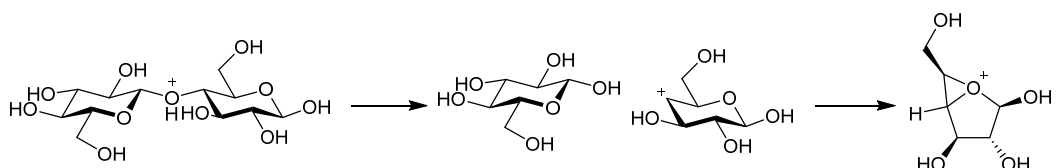


**Fig. S12.** Direct cleavage of a glycosidic bond by tensile force.

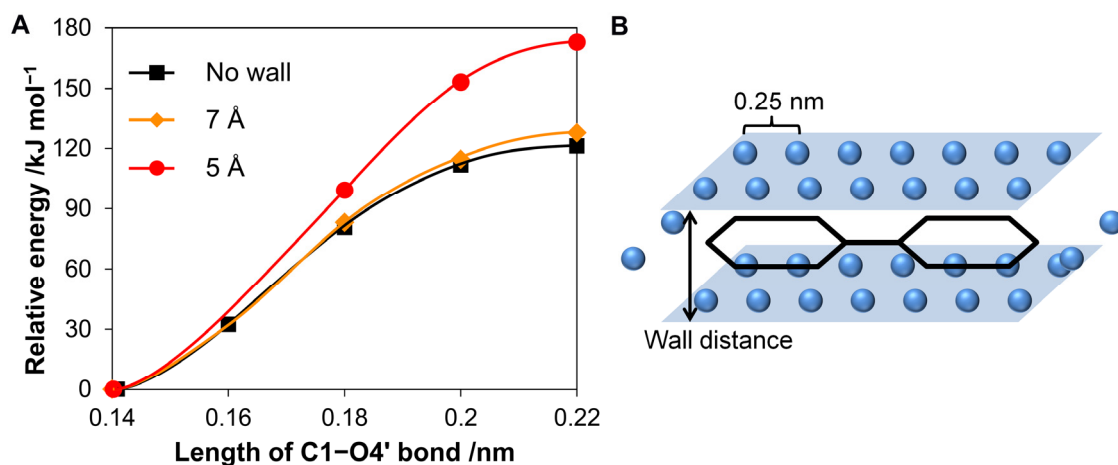


**Fig. S13.** Effect of compression of cellobiose from axial face on the cleavage of glycosidic bond. Cellobiose was pressed with two He walls. The length indicates the distance between the walls. B3LYP-D3/6-31+G(d,p) (C,H,O)/STO-6G (He) was used to give smooth compressive forces in the presence of He walls (D3: S. Grimme, J. Antony, S. Ehrlich and H. Krieg, *J. Chem. Phys.*, 2010, **132**, 154104). He atoms were placed also on the front and back of cellobiose, but they are not shown in Fig. S13B to improve the visibility. As  $\text{H}_3\text{PO}_4$  was located on the cellobiose molecule, He atoms too close to the acid were removed.

To simulate the compression of cellobiose from its axial face, He atoms were placed under and over the molecule. Distance between He atoms was set to 0.25 nm as a slightly shorter distance than twice the van der Waals radius (0.28 nm). To avoid that cellobiose escapes from the sandwiched state, we also put several He atoms on sides, front and back of cellobiose, slightly outside of the van der Waals radii. The front and back He atoms are not shown in Fig. S13B to improve visibility.

This method reproduces that a molecule is pressed in a solid medium with a small additional calculation cost. Another merit is the designability of He arrangement to suit the objective. Complicated points of this method are that the force strength depends on the distance of He atoms within a wall, and the force is inhomogeneous, viz., strong in front of a He atom and weak between two He atoms.

**Table S5.** Atomic coordinate of a transient state for the hydrolysis of cellobiose at the molecular length of no elongation.

O	0	-0.00094500	-0.05481000	-0.55775100
C	0	-1.15554100	-0.87217600	-1.67076300
C	0	-1.56674700	-2.14030900	-0.92473300
C	0	-3.08709100	-2.30775900	-0.89888400
C	0	-3.71113900	-1.00096800	-0.41571600
C	0	-3.40938100	0.13148200	-1.40810800
O	0	-2.07306000	0.04766700	-1.98716100
H	0	-1.22402600	-2.06664100	0.11348400
H	0	-3.44815100	-2.54130200	-1.91353300
H	0	-4.08024800	0.02717100	-2.27817100
H	0	-3.30885100	-0.76278400	0.57528500
H	0	-0.46838400	-1.02852400	-2.49725600
C	0	1.31483400	-0.61026200	-0.62548300
C	0	2.16263300	0.03952700	-1.72736800
C	0	3.61766000	-0.42567800	-1.64542700
C	0	4.18365200	-0.21164100	-0.23619100
O	0	3.35828000	-0.89909300	0.69554300
C	0	2.00140000	-0.40564900	0.74549600
H	0	1.24600500	-1.68804900	-0.81749600
H	0	2.14179200	1.13130900	-1.59494500
H	0	2.01150200	0.66570500	0.99274800
H	0	3.65861200	-1.50297900	-1.87091700
H	0	4.23060300	0.85846200	0.00495000
O	-1	5.49875200	-0.68711600	-0.11568400
H	0	5.48894700	-1.65183000	-0.22073500
C	0	-3.59753700	1.53671100	-0.82397300
H	0	-3.02222200	1.64838800	0.10296600
H	0	-3.22861400	2.27215600	-1.54146000
C	0	1.32013600	-1.14881200	1.88773000
H	0	0.29149800	-0.79597700	1.98127600
H	0	1.85333300	-0.92053400	2.81949600
O	0	-4.97994300	1.82089100	-0.61949800
H	0	-5.35310500	1.14559000	-0.03272300
O	0	1.59905200	-0.29696400	-2.99631800
H	0	2.15468300	0.10264600	-3.68128600
O	0	1.25021700	-2.55950600	1.67828600
H	0	2.15622500	-2.89229100	1.60777700
O	0	-0.91600800	-3.22108300	-1.58351600
H	0	-1.04541900	-4.01654900	-1.04680500
O	0	4.34278400	0.31470500	-2.62463200
H	0	5.26895000	0.03420900	-2.60109400
O	0	-3.36419100	-3.38821000	-0.01906100
H	0	-4.31636600	-3.39907300	0.16009700
O	-1	-5.12482500	-1.12467600	-0.20456500
H	0	-5.56713100	-1.27627000	-1.05475500
H	0	-0.14078900	1.47049900	-0.63788200
O	0	-0.25230200	2.49176200	-0.67929100
P	0	0.08183000	3.29827900	0.63289700
O	0	1.34868100	2.96664100	1.34917600
O	0	-0.02882400	4.84437100	0.17022500
H	0	0.83752000	5.22634300	-0.03699700
O	0	-1.26345900	3.11951400	1.51376800
H	0	-1.16286600	3.44678100	2.42096000

**Table S6.** Atomic coordinate at the maximum electronic energy in the reaction coordinate for the hydrolysis of cellobiose at the molecular length of 9.4% elongation.

O	0	-0.21711100	-0.42495900	0.01300700
C	0	1.36782600	-1.28381900	0.70386300
C	0	2.05471400	-1.83226800	-0.52472800
C	0	3.55095900	-2.09942900	-0.17682000
C	0	4.27415700	-0.77412500	0.11639200
C	0	3.45744600	0.05717100	1.15772500
O	0	2.06692800	-0.45621300	1.44352100
H	0	2.01356200	-1.08291700	-1.32898500
H	0	3.60101400	-2.76565800	0.69855600
H	0	3.91439100	-0.04781100	2.14463100
H	0	4.31490800	-0.22162200	-0.82780500
H	0	0.72848800	-1.94149800	1.28479200
C	0	-1.59086000	-0.94126100	0.11340400
C	0	-2.28899200	-0.56452700	1.42720200
C	0	-3.80829500	-0.90029600	1.41671600
C	0	-4.53291500	-0.29515300	0.19786700
O	0	-3.84165200	-0.79319700	-0.95143400
C	0	-2.44596200	-0.38739100	-1.07164400
H	0	-1.51600200	-2.02888900	0.02781000
H	0	-2.18692700	0.51907000	1.58397300
H	0	-2.38773300	0.70980500	-1.07748100
H	0	-3.92043000	-1.99490700	1.36998700
H	0	-4.49720900	0.80057800	0.22445700
O	-1	-5.93380100	-0.60409400	0.11895400
H	0	-6.02671900	-1.56390400	0.00449400
C	0	3.33372600	1.55139800	0.83421600
H	0	2.90688000	1.70819900	-0.16216600
H	0	2.66452200	2.01522000	1.56021600
C	0	-1.99588600	-0.90172300	-2.43401300
H	0	-0.93877700	-0.66823800	-2.57508800
H	0	-2.57429500	-0.38666000	-3.21123700
O	0	4.60373800	2.17957700	0.97549100
H	0	5.14102300	2.02032300	0.18793900
O	0	-1.63916600	-1.26800800	2.48452000
H	0	-2.05810800	-1.00326200	3.31653000
O	0	-2.12575600	-2.31672400	-2.55924000
H	0	-3.06193200	-2.53281400	-2.44186000
O	0	1.38016400	-3.01346500	-0.89141200
H	0	1.85785000	-3.41214900	-1.63421300
O	0	-4.31399600	-0.40057900	2.65221700
H	0	-5.25206300	-0.62805400	2.72057000
O	0	4.09040900	-2.74691100	-1.31738100
H	0	5.03207200	-2.91507000	-1.16545300
O	-1	5.68937900	-0.94744000	0.45135400
H	0	5.76599100	-1.35639400	1.32787300
H	0	-0.15531900	0.66492400	0.20541700
O	0	-0.06737800	1.95898400	0.43960400
P	0	-0.29357400	3.02072100	-0.64452200
O	0	-1.52931200	2.99536300	-1.50039900
O	0	-0.15036000	4.46094800	0.12175300
H	0	-0.86379200	5.05653600	-0.14974600
O	0	1.07180200	2.94308300	-1.55511300
H	0	0.97561000	3.44199300	-2.37998300

**Table S7.** Atomic coordinate of a transient state for the hydrolysis of cellobiose at the molecular length shortened by 7.5%.

O	0	-0.56633700	0.13888200	-0.03311700
C	0	-0.77270500	-1.62958000	-0.29761000
C	0	-1.40949700	-2.08089600	1.01105000
C	0	-2.91195100	-1.74302900	1.10436300
C	0	-3.45723000	-1.12765000	-0.18692000
C	0	-2.91127600	-1.87762600	-1.40782900
O	0	-1.45364700	-1.79316900	-1.43287300
H	0	-0.89273800	-1.60308900	1.84730300
H	0	-3.42447100	-2.70355400	1.26778200
H	0	-3.17059200	-2.94287700	-1.35060200
H	0	-3.16289100	-0.07671300	-0.24544300
H	0	0.27288400	-1.88605200	-0.44616900
C	0	0.68978800	0.44952800	0.56625200
C	0	1.77527600	0.70600900	-0.48555800
C	0	3.04323000	1.26377000	0.15845600
C	0	2.71871200	2.48541300	1.02701900
O	0	1.76851200	2.10960600	2.01297700
C	0	0.49803900	1.68188500	1.47865300
H	0	1.01560100	-0.38666300	1.19968800
H	0	1.40411500	1.44361800	-1.21159500
H	0	0.04811200	2.50067600	0.89887100
H	0	3.48397000	0.49050500	0.80777200
H	0	2.33556100	3.30981600	0.41101900
O	-1	3.85733500	2.98616600	1.67288600
H	0	4.15635500	2.33003400	2.32223700
C	0	-3.37946600	-1.31627900	-2.75621200
H	0	-3.18685500	-0.23761800	-2.79317400
H	0	-2.80043700	-1.79520600	-3.54983700
C	0	-0.38624000	1.39449400	2.68745000
H	0	-1.36113700	1.03501300	2.35455200
H	0	-0.52297400	2.32622500	3.25106500
O	0	-4.74816600	-1.61575900	-3.00688200
H	0	-5.27154900	-1.16793900	-2.32431900
O	0	2.04412700	-0.52882900	-1.15318800
H	0	2.71751300	-0.36167400	-1.82833600
O	0	0.15539400	0.37306000	3.52884500
H	0	1.01659800	0.68215900	3.84446200
O	0	-1.29195800	-3.50896000	1.08095100
H	0	-0.38203700	-3.74614900	1.30987200
O	0	3.93872500	1.59126200	-0.90067900
H	0	4.74683900	1.96154900	-0.51697500
O	0	-3.11481600	-0.88639600	2.22171200
H	0	-4.05464300	-0.65441000	2.25616000
O	-1	-4.89077200	-1.10535800	-0.17657600
H	0	-5.22732400	-2.00346100	-0.02947300
H	0	-0.99446200	0.99081200	-1.23920600
O	0	-1.31665800	1.56215800	-2.02826000
P	0	-2.03399600	2.91840300	-1.65606500
O	0	-1.36658500	3.80739800	-0.66125100
O	0	-2.30113400	3.61120200	-3.09194500
H	0	-1.62982900	4.27616100	-3.30802800
O	0	-3.51645900	2.42057700	-1.24258700
H	0	-4.04536600	3.11620800	-0.82239600

**Table S8.** Atomic coordinate of a transient state for the hydrolysis of cellobiose compressed by He walls. The distance of He walls was 5 Å.

C	0	3.17978900	-1.91567900	-0.02611400
C	0	1.68059400	-1.71890000	-0.24384200
C	0	1.30315200	-0.37057500	0.32619800
C	0	3.50125000	0.56529100	-0.09678600
C	0	3.87138000	-0.77105300	-0.74141700
H	0	1.49813200	-1.72033000	-1.32356100
H	0	3.40909600	-1.87481100	1.02934800
H	0	3.90966800	0.59514800	0.90360100
H	0	3.51179200	-0.78312600	-1.75644000
H	0	0.95408000	-0.41013200	1.34806700
O	0	-0.23540700	0.12903800	-0.46326200
C	0	-1.35837900	0.33603700	0.40587500
C	0	-1.84995900	1.77831000	0.13525400
C	0	-2.42109900	-0.62886600	-0.06649100
H	0	-1.10223400	0.17371500	1.44061200
C	0	-3.35778400	2.02469700	0.36587700
H	0	-1.65954800	1.95557000	-0.92439900
H	0	-2.47640100	-0.34774200	-1.10050800
C	0	-4.23947500	0.81689500	-0.00887000
H	0	-3.50989500	2.25220100	1.41536300
H	0	-4.26660700	0.70923500	-1.08631600
O	0	2.06498600	0.70327300	0.01161400
O	0	-3.68657400	-0.36717700	0.55092100
O	0	-5.56987300	0.93972100	0.37487600
H	0	-5.63168000	0.99427800	1.33517900
C	0	3.97884400	1.83784000	-0.79786200
H	0	3.61034900	1.89173800	-1.82604900
H	0	3.56341500	2.68097200	-0.24702700
C	0	-2.15304200	-2.12426700	-0.05497500
H	0	-1.13386000	-2.31355000	-0.37715700
H	0	-2.82512200	-2.58632400	-0.78728900
O	0	5.39566900	1.96892500	-0.73447900
H	0	5.79261400	1.20275900	-1.17573600
O	0	-1.14475400	2.77493900	0.88489100
H	0	-0.24662600	2.83259700	0.53142300
O	0	-2.31027100	-2.74265500	1.21215700
H	0	-3.22152300	-2.58822500	1.49016500
O	0	0.90695500	-2.70136700	0.41034100
H	0	1.15418100	-3.56245800	0.04709500
O	0	-3.80815600	3.13010900	-0.41346600
H	0	-3.35641800	3.91170400	-0.07778200
O	0	3.51383200	-3.19806600	-0.53623700
H	0	4.47622900	-3.24477900	-0.63135900
O	0	5.28894700	-0.94748200	-0.80567300
H	0	5.66467800	-0.92756100	0.08658100
H	0	-0.38215800	-0.10850700	-1.98583700
O	0	-0.51139100	-0.16241400	-2.99488300
P	0	-0.34589200	-1.57964700	-3.66690000
O	0	-1.11486400	-2.72711200	-3.11185100
O	0	-0.64270300	-1.27455000	-5.22631200
H	0	-1.49907000	-1.63556000	-5.50108000
O	0	1.26418600	-1.78347700	-3.64308800
H	0	1.51998700	-2.68783800	-3.88214800
He	-1	-4.81729900	1.76227600	2.78577000
He	-1	-2.70730300	-1.00908600	2.75635500
He	-1	0.10572500	0.96519000	2.48482800
He	-1	2.57282000	0.58646600	2.34302100
He	-1	5.02865300	0.14800400	2.17983300
He	-1	-5.18143500	-0.78371400	2.94495800
He	-1	-2.34002600	1.45929700	2.64004500
He	-1	-0.26105600	-1.50436500	2.61266600
He	-1	2.20177500	-1.88501900	2.41399300
He	-1	4.65793300	-2.32350500	2.25623900
He	-1	-2.50431000	5.36486000	1.68518200
He	-1	0.47756900	5.07036200	1.53775600
He	-1	3.43317600	4.60222100	1.32631000
He	-1	-5.34198400	1.76484500	-2.18660700
He	-1	-3.23198000	-1.00640900	-2.21598900
He	-1	2.04809400	0.58899800	-2.62944700
He	-1	4.50389600	0.15048200	-2.79253100
He	-1	-5.70612400	-0.78115200	-2.02743000
He	-1	-2.86464300	1.46189100	-2.33234500
He	-1	4.13327500	-2.32091200	-2.71618000
He	-1	-3.88723700	-4.53569500	1.94172700
He	-1	-0.90541100	-4.83022000	1.79432500
He	-1	2.05040900	-5.29824100	1.58268500
He	-1	-2.63783200	5.35831300	-0.81767900
He	-1	0.34403700	5.06384800	-0.96508400
He	-1	3.29975200	4.59544100	-1.17655500
He	-1	-4.10881000	-4.53038100	-0.59626800
He	-1	-1.12694500	-4.82488600	-0.74368300
He	-1	1.82856800	-5.29315400	-0.95524000
He	-1	-7.78293700	2.30712300	0.38177200
He	-1	-8.19079600	-0.40213200	0.50136700
He	-1	7.97172600	-0.39739600	-0.30826500
He	-1	7.59874500	-2.87585500	-0.25443100